



PERGAMON

Journal of Quantitative Spectroscopy &
Radiative Transfer 74 (2002) 767–781

Journal of
Quantitative
Spectroscopy &
Radiative
Transfer

www.elsevier.com/locate/jqsrt

Extension of the discrete-ordinate algorithm and efficient radiative transfer calculation

Yi Qin^a, David L.B. Jupp^b, Michael A. Box^{a,*}

^a*School of Physics, University of New South Wales, Sydney, NSW 2052, Australia*

^b*Earth Observation Center, CSIRO, Canberra, ACT 2601, Australia*

Received 6 August 2001; accepted 23 November 2001

Abstract

As an accurate and efficient algorithm, the discrete-ordinate method (DOM) has been used to solve the radiative transfer problem of plane-parallel scattering atmosphere illuminated by a parallel beam, an idealized case of the sun, from above the atmosphere. In this paper, we extend this algorithm so that radiative problems of more general sources, such as parallel surface sources that illuminate with a parallel beam in any direction from any vertical position, and general surface sources that illuminate continuously in a hemisphere, can be solved. For a problem where intensity distributions are sought for a number of different sources within the same atmosphere-surface system, the intrinsic properties of DOM are used so that the time required for the solution for extra sources is reduced to a substantially small amount. In the case of parallel surface sources, numerical testing has shown that the amount can be reduced to as little as 15% of a full solution. Examples of applications are presented. © 2002 Published by Elsevier Science Ltd.

Keywords: Radiative transfer; Adjoint formulation; Radiative perturbation theory

1. Introduction

In a previous paper [1], the radiative perturbation theory [2,3] was used to establish a linear system based on the method of Sendra and Box [4,5] to represent approximately the relation between atmospheric optical properties and exiting radiance. This linear system can then be inverted so that the atmospheric optical properties could be retrieved. However, the perturbation theory may require that an adjoint problem be solved for each observation [2,3], and the adjoint source of an adjoint problem may be an arbitrary function of altitude (optical thickness), zenith angle and azimuth angle. For example, in the case of intensity observation, the adjoint source may be expressed as $\delta(\tau - \tau_{\text{obs}})\delta(\Omega - \Omega_{\text{obs}})$, which corresponds to an observation of intensity at optical thickness τ_{obs} and

* Corresponding author. Tel.: +612-9385-4545; fax: +612-9385-6060.

E-mail address: m.box@unsw.edu.au (M.A. Box).

in the direction of Ω_{obs} . We note that τ_{obs} and Ω_{obs} are almost arbitrary: τ_{obs} could be any value between 0 and τ_a —the total optical thickness—and Ω_{obs} could be upward or downward. Another example is flux observation at the ground. In this case, the adjoint source becomes a continuous function of solid angle in the upper hemisphere. Because of such requirement by the perturbation theory, it is necessary to extend radiative transfer algorithms to deal with arbitrary adjoint sources so that the theory can be applied in our inversion, and in other applications.

In the case of CIMEL Sunphotometer measurements [6], a principal plane scan takes as many as 40 observations, which means up to 40 radiative transfer solutions may be needed. Because of the approximation involved in the linear relation [3], iteration is also required. Both reasons require measures be taken to reduce the amount of computation. However, in the case of almucantar circle scan (and the surface reflectance is assumed to be azimuthally independent), we do not need to solve the radiative transfer equation for each observation angle because the zenith angles of all observations are the same. The discussion about principal plane scan thus does not apply to this case.

As an accurate as well as effective algorithm, starting with its original derivation by Chandrasekhar [7], the discrete-ordinate method (DOM) has been well developed by a number of authors. Among them are Liou [8,9], who extended this method to vertically variable atmospheres and introduced the matrix method, Asano [10], who pointed out the way to reduce the order of the eigenvalue problem by half, Stamnes and Swanson [11], who restated these ideas more clearly so that numerical implementation became easier, and Stamnes and Conklin [12], who introduced a scaling scheme to avoid overflow while determining the integration constants, so that the algorithm becomes more stable.

In the category of accurate radiative transfer algorithms, the DOM can provide the most flexible trade-off between precision and computation time. Most importantly, it has the natural properties that can lead to significant efficiency improvement when multiple (different) sources are considered for the same atmosphere-surface system. Because of this, this algorithm is most suitable for sky radiance inversion based on perturbation theory. However, for each new type of source, special extension is required, and a rather significant amount of programming is usually required.

In this paper, we will extend the DOM algorithm first. Then we will discuss the simultaneous solution of multi-source problems and show how much time can be saved. After that we present example applications of our program, especially on how to apply the Green's function and the general principle of reciprocity to perform high efficiency radiative transfer calculations.

2. Extended discrete-ordinate algorithm for multi-source radiative transfer problems

We will start the extension on the basis of Stamnes and Swanson [11]. However, because the extension happens from place to place, also to maintain the integrity of the paper, we will try to give a complete outline of the algorithm but some detailed steps may be omitted. Matrix notation will be adopted where possible, as it leads to much more concise expressions.

2.1. Extended sources and corresponding radiative transfer equations

The first type of extended source is a parallel surface source (PSS). By “surface” it means the source illuminates at a fixed vertical position (measured by optical thickness here) in a given

direction, and extends infinitely in horizontal directions. If a PSS illuminates towards the lower boundary, we call it a downward PSS and it is defined by $I_d(\tau_d, -\mu_d, \phi_d)$. Here we use “-” to indicate a direction towards the lower boundary. In parallel, we have an upward PSS defined by $I_u(\tau_u, \mu_u, \phi_u)$. The sun is then a special case of the downward PSS. We use subscripts “d” and “u” to distinguish I , μ and ϕ between these two cases. These subscripts are also applied to τ because there is a necessity to distinguish it later in transmittance equations, Eqs. (5) and (6).

Another type of extended source is a general surface source (GSS). We use “general” to indicate that GSS illuminates in all directions within a hemisphere. In this paper, we limit GSS to be: (1) located at the lower boundary; (2) illuminating in the upper hemisphere and; (3) azimuthally symmetrical. Such a surface source is thus completely described by $I_s(\mu, \phi)$ and may be referred as the ground GSS.

In this paper, the reflection by the lower boundary is defined by a general bi-directional reflectance function, $A_s(-\mu', \phi'; \mu, \phi)$, with the assumption that it is azimuthally symmetrical, where (μ, ϕ) and $(-\mu', \phi')$ are the reflected and incident directions, respectively.

The atmosphere is approximated as a series of homogeneous sub-layers numbered from the top to the bottom [9]. Each sub-layer is defined by $\{\tau_l, \tilde{\omega}_l, P_l(\mu, \phi; \mu', \phi'); l = 1, 2, \dots, N_l\}$, where τ_l is the optical depth at the bottom of this sub-layer, so the first sub-layer is between 0 and τ_1 , the second sub-layer is between τ_1 and τ_2 and so on. $\tilde{\omega}_l$ is the single scattering albedo and P_l is the phase function. The total optical depth is denoted as τ_a which equals τ_{N_l} . Each sub-layer will be solved independently at first, and results finally connected through continuity conditions.

Taking into account of all the three types of source, the radiative transfer equation within a sub-layer becomes

$$\mu \frac{dI(\tau, \mu, \phi)}{d\tau} = I(\tau, \mu, \phi) - \frac{\tilde{\omega}}{4\pi} \int_0^{2\pi} \int_{-1}^1 P(\tau; \mu, \phi, \mu', \phi') I(\tau, \mu', \phi') d\mu' d\phi' - Q(\tau, \mu, \phi), \quad (1)$$

where $Q(\tau, \mu, \phi)$ depends on the type of source

$$Q_u(\tau, \mu, \phi) = \frac{\tilde{\omega}}{4\pi} I_u P(\tau; \mu, \phi; \mu_u, \phi_u) t_u(\tau), \quad (2)$$

$$Q_d(\tau, \mu, \phi) = \frac{\tilde{\omega}}{4\pi} I_d P(\tau; \mu, \phi; -\mu_d, \phi_d) t_d(\tau), \quad (3)$$

$$Q_g(\tau, \mu, \phi) = \frac{\tilde{\omega}}{4\pi} \int_0^{2\pi} \int_0^1 P(\tau; \mu, \phi, \mu', \phi') I_s(\mu', \phi') t_s(\tau, \mu') d\mu' d\phi', \quad (4)$$

respectively, for the upward PSS, the downward PSS and the ground GSS. In these equations

$$t_u(\tau) = U(\tau_u - \tau) e^{-(\tau_u - \tau)/\mu_u}, \quad (5)$$

$$t_d(\tau) = U(\tau - \tau_d) e^{-(\tau - \tau_d)/\mu_d}, \quad (6)$$

$$t_s(\tau, \mu) = e^{-(\tau_a - \tau)/\mu} \quad (7)$$

are transmittance equations defined for the three types of source. $U(x)$ is defined as

$$U(x) = \begin{cases} 1, & x \geq 0, \\ 0, & x < 0. \end{cases} \quad (8)$$

Eqs. (1)–(7) are derived in a similar way to Liou [13] for the case of solar illumination. For simplicity, layer number is omitted until Section 2.5, where boundary and continuity conditions are used to determine the integration constants.

2.2. Discrete radiative transfer equation and its matrix form

Following the matrix approach [11,13], we first expand the intensity, $I(\tau, \mu, \phi)$, and the ground GSS, $I_s(\mu, \phi)$, into Fourier series of order $2N_i - 1$

$$I(\tau, \mu, \phi) = \sum_{m=0}^{2N_i-1} I^m(\tau, \mu) \cos m(\phi_0 - \phi), \quad (9)$$

$$I_s(\mu, \phi) = \sum_{m=0}^{2N_i-1} I_s^m(\mu) \cos m(\phi_0 - \phi), \quad (10)$$

where ϕ_0 is a reference azimuth. The phase function is expanded into Legendre polynomials according to

$$P(\Theta) = \sum_{j=0}^{2N_i-1} \chi_j P_j(\cos(\Theta)), \quad (11)$$

where $\cos(\Theta) = \mu\mu' + (1 - \mu^2)^{1/2}(1 - \mu'^2)^{1/2} \cos(\phi - \phi')$ is the cosine of the scattering angle. It has been shown by Liou [13] that

$$P(\mu, \phi; \mu', \phi') = \sum_{j=0}^{2N_i-1} \sum_{m=0}^j \chi_j^m P_j^m(\mu) P_j^m(\mu') \cos m(\phi - \phi'), \quad (12)$$

$$\chi_j^m = (2 - \delta_{0,m}) \frac{(j-m)!}{(j+m)!} \chi_j,$$

where $P_j^m(\mu)$ are associated Legendre functions.

To discretize the radiative transfer equation, we represent the m th Fourier component of the intensity, $I^m(\tau, \mu)$, by two vectors of N_s elements, $\mathbf{I}_{\pm}^m = [I^m(\tau, \pm\mu_1), \dots, I^m(\tau, \pm\mu_{N_s})]^T$, and represent the m th component of the ground GSS, $I_s^m(\mu)$, by a vector of N_s element, $[I_s^m(\mu_1), \dots, I_s^m(\mu_{N_s})]$.

Considering the orthogonality of Legendre polynomials, by inserting Eqs. (9) and (12) into Eq. (1) and grouping the resulting equation by $\cos m(\phi - \phi_0)$, Eq. (1) can be separated into $2N_i$ independent equations corresponding to the $2N_i$ Fourier components of intensity. Finally, we substitute integration

over zenith angle by Gaussian quadrature, for example

$$\int_{-1}^1 P_j^m(\mu') I^m(\tau; \mu') d\mu' = \sum_{i=-N_s, i \neq 0}^{N_s} a_i P_j^m(\mu_i) I^m(\tau; \mu_i), \quad (13)$$

where a_i and μ_i are the Gaussian quadrature weights and points, and $a_{-i} = a_i$, $\mu_{-i} = -\mu_i$. We get for each of the Fourier component of intensity the discrete ordinate equation which is written in matrix form as [11,13]:

$$\begin{bmatrix} \mathbf{U} & \mathbf{0} \\ \mathbf{0} & -\mathbf{U} \end{bmatrix} \frac{d}{d\tau} \begin{bmatrix} \mathbf{I}_+^m \\ \mathbf{I}_-^m \end{bmatrix} = \begin{bmatrix} \mathbf{E} - \mathbf{C}_{++}^m & -\mathbf{C}_{+-}^m \\ -\mathbf{C}_{-+}^m & \mathbf{E} - \mathbf{C}_{--}^m \end{bmatrix} \begin{bmatrix} \mathbf{I}_+^m \\ \mathbf{I}_-^m \end{bmatrix} - \begin{bmatrix} \mathbf{S}_+^m \\ \mathbf{S}_-^m \end{bmatrix}. \quad (14)$$

In the above equation, $\mathbf{U} = \text{diag}(\mu_1, \dots, \mu_{N_s})$, \mathbf{E} is the $N_s \times N_s$ identity matrix, the \mathbf{C} 's are $N_s \times N_s$ matrices of elements:

$$C_{ij}^m = (1 + \delta_{0m}) \frac{\tilde{\omega}}{4} a_j \sum_{k=m}^{2N_s-1} \chi_k^m P_k^m(\mu_i) P_k^m(\mu_j), \quad i, j = \pm 1, \pm 2, \dots, \pm N_s. \quad (15)$$

Note that $C_{-ij}^m = C_{i-j}^m$, $C_{-i-j}^m = C_{ij}^m$, and C_{xy} is symmetric. The signs of i, j in Eq. (15) corresponds to x, y in \mathbf{C}_{xy} .

S_{\pm} are N_s -element vectors that depend on the type of source. For the upward PSS, the downward PSS and the ground GSS, respectively, the i th element, $i = \pm 1, \dots, \pm N_s$, is

$$S_i^m = C_u^m(\mu_i) t_u(\tau), \quad (16)$$

where

$$C_u^m(\mu_i) = \frac{\tilde{\omega}}{4\pi} I_u \sum_{k=m}^{2N_i-1} \chi_k^m P_k^m(\mu_i) P_k^m(\mu_u), \quad (17)$$

$$S_i^m = C_d^m(\mu_i) t_d(\tau), \quad (18)$$

where

$$C_d^m(\mu_i) = \frac{\tilde{\omega}}{4\pi} I_d \sum_{k=m}^{2N_i-1} \chi_k^m P_k^m(\mu_i) P_k^m(-\mu_d), \quad (19)$$

$$S_i^m = \sum_{k=1}^{N_s} C_{sk}^m(\mu_i) t_s(\tau, \mu_k), \quad (20)$$

where

$$C_{sk}^m(\mu_i) = C_{ik}^m I_s^m(\mu_k). \quad (21)$$

2.3. General solution

The problem now is to solve for each sub-layer and Fourier component of intensity, i.e., in total $N_1 \times 2N_i$ discrete ordinate equations, Eq. (14). Because the homogeneous part is source independent,

the general solution needs be solved only once and the result is applicable to all sources. Seeking a solution of the following form to the homogeneous part of Eq. (14):

$$\mathbf{I}_{\pm} = \mathbf{\Phi}_{\pm} e^{-\lambda\tau} \quad (22)$$

leads to [11]

$$(\mathbf{X} - \mathbf{Y})(\mathbf{X} + \mathbf{Y})(\mathbf{\Phi}_{+} + \mathbf{\Phi}_{-}) = \lambda^2(\mathbf{\Phi}_{+} + \mathbf{\Phi}_{-}), \quad (23)$$

$$(\mathbf{X} + \mathbf{Y})(\mathbf{\Phi}_{+} + \mathbf{\Phi}_{-}) = \lambda(\mathbf{\Phi}_{+} - \mathbf{\Phi}_{-}), \quad (24)$$

where $\mathbf{X} = \mathbf{U}^{-1}(\mathbf{C}_{++} - \mathbf{E})$ and $\mathbf{Y} = \mathbf{U}^{-1}\mathbf{C}_{+-}$. Eq. (23) is a standard eigenvalue problem which can be solved by standard library routines readily available from many sources. Together with Eq. (24), all the eigenvectors and values, $\mathbf{\Phi}_{\pm}$ and λ , can be obtained.

2.4. Particular solutions

For each type of source, the particular solution to Eq. (14), \mathbf{I}_p , needs be calculated separately. For an upward PSS and downward PSS we seek, respectively,

$$\mathbf{I}_p = \mathbf{Z}_u t_u(\tau), \quad (25)$$

$$\mathbf{I}_p = \mathbf{Z}_d t_d(\tau). \quad (26)$$

For the ground GSS, each discrete stream, $I_s^m(\mu_k)$ as in Eq. (20), must be solved one by one. We seek

$$\mathbf{I}_{pk} = \mathbf{Z}_{sk} t_s(\tau, \mu_k), \quad k = 1, 2, \dots, N_s. \quad (27)$$

Eqs. (25)–(27) lead to

$$\left(\tilde{\mathbf{E}} - \mathbf{C} - \frac{\tilde{\mathbf{U}}}{\mu_u} \right) \mathbf{Z}_u = \mathbf{C}_u, \quad (28)$$

$$\left(\tilde{\mathbf{E}} - \mathbf{C} + \frac{\tilde{\mathbf{U}}}{\mu_d} \right) \mathbf{Z}_d = \mathbf{C}_d \quad (29)$$

and

$$\left(\tilde{\mathbf{E}} - \mathbf{C} - \frac{\tilde{\mathbf{U}}}{\mu_k} \right) \mathbf{Z}_{sk} = \mathbf{C}_{sk}, \quad k = 1, 2, \dots, N_s, \quad (30)$$

where

$$\mathbf{C} = \begin{bmatrix} \mathbf{C}_{++} & \mathbf{C}_{+-} \\ \mathbf{C}_{+-} & \mathbf{C}_{++} \end{bmatrix}, \quad \tilde{\mathbf{U}} = \begin{bmatrix} \mathbf{U} & \mathbf{0} \\ \mathbf{0} & -\mathbf{U} \end{bmatrix},$$

$\tilde{\mathbf{E}}$ is $2N_s \times 2N_s$ identity matrix, and $\mathbf{C}_{u/d} = [C_{u/d}^m(\mu_1), \dots, C_{u/d}^m(\mu_{N_s}), C_{u/d}^m(-\mu_1), \dots, C_{u/d}^m(-\mu_{N_s})]^T$. $\mathbf{Z}_u, \mathbf{Z}_d$ and \mathbf{Z}_{sk} can then be solved for, and the particular solution found.

2.5. The complete solution

The complete solution in the l th sub-layer can now be written as

$$\mathbf{I}^l(\tau) = \mathbf{\Phi}^l \mathbf{\Lambda}^l(\tau) \mathbf{L}^l + \mathbf{H}^l(\tau). \tag{31}$$

From this section on, a superscript ‘ l ’ is used to indicate the sub-layer. In Eq. (31),

$$\mathbf{I}^l = \begin{bmatrix} \mathbf{I}_+^l \\ \mathbf{I}_-^l \end{bmatrix}, \quad \mathbf{\Phi}^l = \begin{bmatrix} \mathbf{\Phi}_+^l & \mathbf{\Phi}_-^l \\ \mathbf{\Phi}_-^l & \mathbf{\Phi}_+^l \end{bmatrix},$$

$\mathbf{\Lambda}^l(\tau) = \text{diag}(\exp(-\lambda_i^l \tau), i = 1, 2, \dots, N_s, -1, -2, \dots, -N_s)$ and

$$\mathbf{H}^l(\tau) = \begin{cases} \mathbf{Z}_u^l t_u(\tau) & \text{for upward PSS,} \\ \mathbf{Z}_d^l t_d(\tau) & \text{for downward PSS,} \\ \sum_{k=1}^{N_s} \mathbf{Z}_{sk}^l t_s(\tau, \mu_k) & \text{for ground GSS.} \end{cases} \tag{32}$$

The integration constant vector, \mathbf{L}^l , is to be determined from boundary conditions. In matrix form, the upper boundary condition is written as

$$\mathbf{I}_-^l(0) = \mathbf{0} \tag{33}$$

in which the subscript ‘ $-$ ’ indicates the lower hemisphere. The lower boundary condition is written as

$$\mathbf{I}_+^{N_s}(\tau_a) = \mathbf{B} \mathbf{I}_-^{N_l}(\tau_a) + \mathbf{R} \tag{34}$$

in which the subscript ‘ $+$ ’ indicates the upper hemisphere. $\mathbf{B} \in R^{2N_s \times 2N_s}$ is defined as

$$B_{ij} = (1 + \delta_{0m}) a_j \mu_j A_s^m(\mu_i, -\mu_j), \quad i, j = \pm 1, \pm 2, \dots, \pm N_s, \tag{35}$$

where A_s^m is defined via

$$A_s(-\mu', \phi'; \mu, \phi) = \sum_{m=0}^{2N_s-1} A_s^m(\mu, -\mu') \cos m(\phi' - \phi). \tag{36}$$

The N_s -element column vector, \mathbf{R} , exist only in the case of a downward PSS (including the solar beam case) and its elements are defined by

$$R_i = \frac{\mu_d I_d t_d(\tau_a)}{\pi} A_s^m(\mu_i, -\mu_d), \quad i = 1, 2, \dots, N_s. \tag{37}$$

Between the l th and $(l + 1)$ th sub-layers, the intensity satisfies the continuity condition

$$\mathbf{I}_\pm^l(\tau_l) = \mathbf{I}_\pm^{l+1}(\tau_l), \quad l = 1, 2, \dots, N_l - 1, \tag{38}$$

where τ_l is the optical depth at the boundary of the l th and $(l + 1)$ th sub-layer.

general principle of reciprocity [14,15]. Briefly, the Green’s function $G(\tau, \Omega; \tau', \Omega')$ is the intensity at (τ, Ω) due to a parallel surface source of unit flux, or $1/\mu'$ intensity, at (τ', Ω') . The general principle of reciprocity then is stated as

$$G(\tau, \Omega; \tau', \Omega') = G(\tau', -\Omega'; \tau, -\Omega). \tag{44}$$

Using the linearity of atmospheric radiative transfer, the principle can be extended to any source and any effect.

3.1. Intensity distribution with explicit surface albedo

In the case that the surface is a Lambertian reflector, Liou [13] derived the expression for exiting intensity, at the top and bottom of atmosphere, with the surface albedo explicitly included. In this section, we present a general form of the expression for any optical thickness rather than at the top or bottom of the atmosphere only, and show the method to calculate them efficiently using the extended algorithm.

The intensity at any optical thickness, $0 \leq \tau \leq \tau_a$ where τ_a is the total optical thickness, can be decomposed into two components: (1) the intensity due to the source for the case of $A = 0$; (2) the intensity due to the reflected radiation by the surface, which should be azimuthally independent as will be shown later

$$I^*(\tau, \mu, \phi) = I(\tau, \mu, \phi) + I_g(\tau, \mu), \tag{45}$$

where the first component, $I(\tau, \mu, \phi)$, can be obtained by solving the standard problem (i.e., without surface reflection).

Under the assumption that the surface is a Lambertian reflector, the intensity reflected by the ground, treated as the source of the second component here, is constant over the upper hemisphere. We thus can write it as $I_s(A)U(\mu)$, where A is the surface albedo and $U(\mu) = 1$, where $\mu > 0$ or 0 otherwise. By applying the linearity of atmospheric radiative transfer, we extend the Green’s function to define the following functions:

$$t(\tau, \mu) = \int_0^{2\pi} d(\phi - \phi') \int_0^1 G(\tau, \mu, \phi; \tau_a, \mu', \phi') U(\mu') d\mu', \tag{46}$$

$$r(\tau, \mu) = \int_0^{2\pi} d(\phi - \phi') \int_0^1 G(\tau, -\mu, \phi; \tau_a, \mu', \phi') U(\mu') d\mu'. \tag{47}$$

In these equations, $t(\tau, \mu)$ and $r(\tau, \mu)$ are actually the intensity due to a general surface source, $U(\mu)$, located at the ground. So $t(\tau, \mu)$ and $r(\tau, \mu)$ can be directly computed, without computing the Green’s function first, using the extended algorithm as described in Section 2. Note that they are azimuthally independent, so only the 0th Fourier component is required. The second component thus can be written as

$$I_g(\tau, \mu) = I_s(A)[t(\tau, \mu) + e^{-(\tau_a - \tau)/\mu}], \tag{48}$$

$$I_g(\tau, -\mu) = I_s(A)r(\tau, \mu). \tag{49}$$

In Eq. (48) the term $e^{-(\tau_a-\tau)/\mu}$ must be included to account for the part directly transmitted from the ground.

Finally by following a similar procedure to Liou [13], it can be derived that

$$I_s(A) = \frac{1}{\pi} \frac{A}{1 - A\bar{r}} (F_{\text{dif}}^{\downarrow} + F_{\text{dir}}^{\downarrow}), \quad (50)$$

where $\bar{r} = 2 \int_0^1 r(\tau_a, \mu) \mu d\mu$, $F_{\text{dif}}^{\downarrow}$ is the total downward diffuse flux at the ground for the standard problem, which can be simply calculated as $F_{\text{dif}}^{\downarrow} = \mu_0 I_0 t(0, \mu_0)$, and $F_{\text{dir}}^{\downarrow} = \mu_0 I_0 e^{-\tau_a/\mu_0}$, where μ_0 and I_0 are the cosine of solar zenith angle and solar intensity.

At this point, we have derived the expression which includes the surface albedo explicitly and all the other required values can be calculated. The whole problem requires two solutions of the radiative transfer: the full solution of the standard problem and the 0th Fourier component of the problem due to a general surface source at the ground, $U(\mu)$.

3.2. Simulation of an unrestricted GSS

Using the Green's function and the general principle of reciprocity, we can, by solving the radiative transfer equation only once, compute a particular radiative effect of the same atmosphere-surface system for a number of sources: for example, the computation of net flux passing through a horizontal plane for a range of solar zenith angles. If the plane is at the ground, we can readily do it using the built-in ground GSS. Here, we present a method to simulate an unrestricted (in the vertical position and the illuminating direction) general surface source using parallel surface sources.

Eq. (32) shows that the m th Fourier component of the solution due to a general surface source is the integration over zenith of that due to the discrete streams of the general surface source. Actually, this is just an extension of the linearity of atmospheric radiative transfer. By comparing Eq. (20) with Eq. (16) or Eq. (18), it is seen that

$$I_{\text{GSS}}^m(\tau, \mu) = (1 + \delta_{0m}) \pi \sum_{j=1}^{N_s} a_j I_j^m(\tau, \mu), \quad (51)$$

where $I_j^m(\tau, \mu)$ is the solution of Eq. (14) due to $I_s^m(\tau, \mu_j)$ —the j th stream of the m th Fourier component of the general surface source, which is similar to $I_s^m(\mu_j)$ in Eq. (10) but with the restriction on optical thickness and direction of illumination removed. We can expect that the time used for such a simulation will be only slightly more than when solving for a built-in general surface source.

4. Computer program

The extended algorithm has been implemented in Fortran 90. In this section, we discuss the methods to reduce the time used in solving for extra sources, and some other points that may need attention while implementing the algorithm. To demonstrate the ability in time saving, the timing results of a typical case are reported later in this section.

Table 1
Time (in seconds) used to solve one or more source radiative transfer problem

Number of sources	1	5	20	40
General solution	11.05	11.04	10.56	11.33
Particular solutions	2.76	13.55	52.84	110.08
Integration constants	6.56	7.96	12.46	19.07
Others	0.07	0.08	0.17	0.26
Total	20.44	32.63	76.03	140.74

4.1. Implementation considerations

We have noticed in Section 2.3 that the general solution does not depend on the source, thus it should be solved only once and reused for all the sources in question. Because an eigenvalue problem is very time consuming, this leads to significant improvement for a multi-source radiative transfer problem. The more sources which are solved together, the more benefit we get from the reuse of the general solution.

While determining the integration constants in Section 2.5, because the coefficient matrix does not depend on source, all the integration constants equation system can be merged into a single equation system as in Eq. (40). No matter what method is used to solve this combined equation system, the coefficient matrix, \mathbf{A} , will need to be processed only once. This will lead to further time saving when multiple sources are involved.

Because of the special function $U(x)$ in Eqs. (5)–(7), any layer that has an internal source, a source that is not located exactly on the boundaries, has to be split where the source is located. The general solution in the split layers does not change and thus may also be reused.

Although adjustments have been taken to avoid overflow as in Eq. (39), if one sub-layer is still too thick—say its optical thickness is larger than 20—then overflow may possibly occur. One way around to this problem is to split this thick layer into two or more layers that have the same single scattering albedo and phase function. The general solution again should be reused.

4.2. Timing

Test cases were run to demonstrate the ability of the implemented code on time saving. Some general controlling parameters used in the testing cases are: $N_s = 48$ or 96 streams, $N_i = 48$, $N_l = 1$. The system is Windows 2000 Professional running on AMD K6 233 MHz single CPU system with 96 MB physical memory. The code is compiled by Digital Visual Fortran v6.0 and optimized at full level. The number of sources is increased from 1 to 40. The general solution, particular solution and integration constants are timed separately but the total time is also recorded which is slightly higher than the sum of the three parts. Results are summarized in Table 1. All times are in seconds.

In the case of a single source, the largest contribution (about 54%) to the total time comes from the general solution. As expected, this time does not increase with the number of sources, and thus leads to the most significant time saving. The second largest contribution (32%) is the calculation of the integration constants, including the generation of matrix \mathbf{A} of Eq. (41). This time increases

Table 2

Input parameters for comparison with the doubling and adding code of Evans and Stephens [16]

Parameter	Value
Atmospheric model	Single homogeneous layer
Optical thickness	1.2
Single scattering albedo	0.825
Phase function	Deirmendjian's Haze M aerosol model
Direct solar flux	1.0
Solar zenith	40°
Surface albedo	0.0
Number of streams	32
Order of azimuth expansion	31

slightly with the number of sources at a rate of about 5% for each extra source. The least time consuming among the three in the case of a single source is the particular solution. However, this part is proportional to the number of sources. Because of this, this time component increases linearly with the number of sources. Roughly, after the first source, each extra source will add about 15% to the time for a full solution.

4.3. Numerical testing

As a validation procedure, a number of testing runs have been conducted. We first compared this program with the doubling and adding program by Evans and Stephens [16]. Care has been taken to match input of both programs as exactly as possible, especially the number of streams and the order of azimuth expansion, as both have a significant effect on the precision of computation. The input parameters for both programs are shown in Table 2. The exiting intensity as function of zenith and azimuth at the ground is shown in Fig. 1, where a negative zenith indicates the observation angle is opposite to the sun. In Fig. 2, we show the relative difference of exiting intensities at the top and bottom of the atmosphere calculated by the two programs. A three-layer atmospheric model with non-black surface was also tested but there is no need to present the result here. In both cases, the differences of exiting intensity at both the ground and the top of the atmosphere were $< 0.3\%$, and mostly $< 0.1\%$.

We have also tested the simulation shown in Section 3.2. That is, we compute the intensity distribution due to a ground GSS, such as $U(\mu)$ or $\mu U(\mu)$, using the built-in ground GSS as well as the simulation method. The results were identical as expected.

Finally, we used the general principle of reciprocity to validate our program. That is, we computed $G(\tau, \Omega; \tau', \Omega')$ and $G(\tau', -\Omega'; \tau, -\Omega)$ for a number of $(\tau, \Omega; \tau', \Omega')$ pairs, including τ and τ' that are inside the atmosphere, to see if they are equal to each other. It was found that the error is only due to interpolation of zenith angles if they are not exactly at the Gauss points. This procedure has validated the internal parallel surface source and, indirectly, the general surface source.

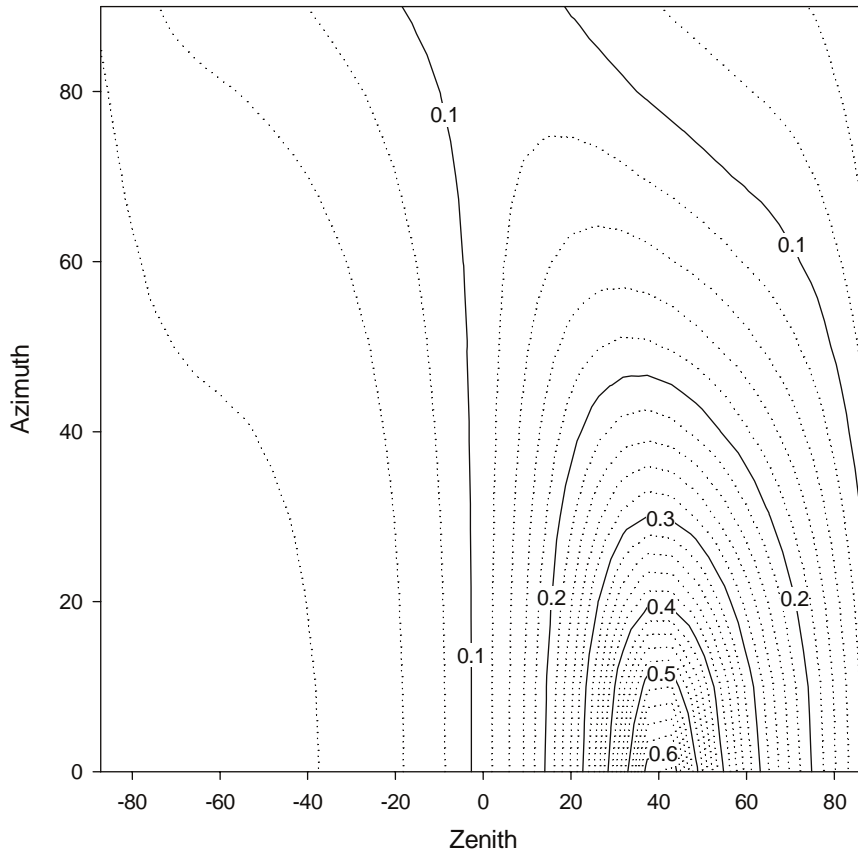


Fig. 1. Intensity distribution at the ground.

5. Conclusion

The discrete-ordinate algorithm for parallel plane atmospheric radiative transfer problems has been extended for more general sources. The first source is a parallel surface source, PSS, which illuminates with a parallel beam from any vertical position and in any direction. The second type is general surface source, GSS, which illuminates in the upper hemisphere as a continuous function of direction. Although we have restricted the GSS to be at the ground, and illuminating only in the upper hemisphere, such restrictions can be removed using the simulation method described in Section 3.2. A Fortran 90 code has been written and has been validated via a number of numerical tests.

We have also discussed methods to improve computation efficiency for radiative problems of multiple sources with the same atmosphere-surface system. Numerical test has shown that, for an extra parallel surface source, only about 15% of the time of a full solution is required by our implemented code. In the case of sky radiance inversion using perturbation theory [1], such improvement has been found essential.

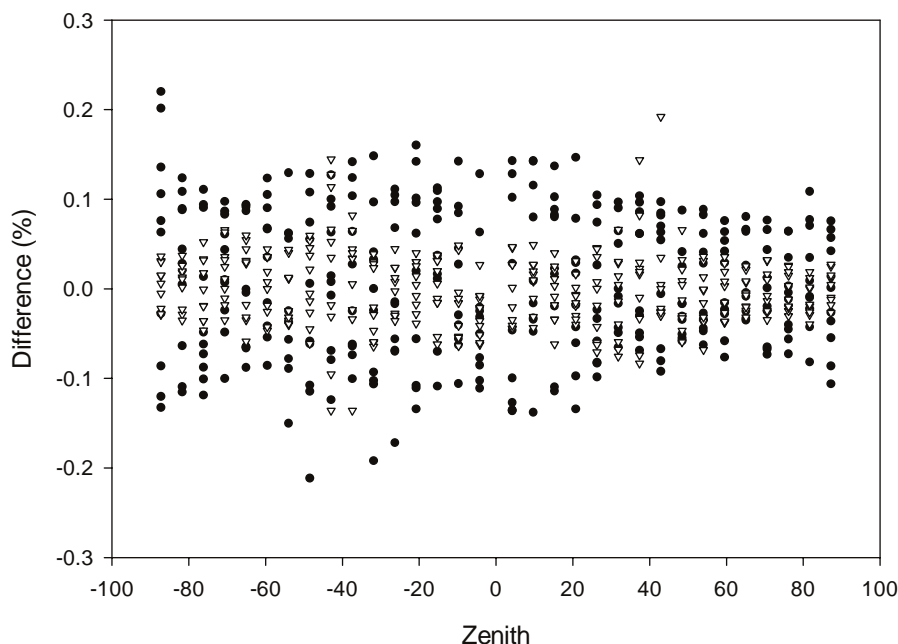


Fig. 2. Relative difference (%) of exiting intensity at the top (circles) and bottom (triangles) of atmosphere calculated by our program and that of Evans and Stephens.

As well as for perturbation calculations, the extended algorithm is also a useful tool to perform efficient radiative transfer calculations. We have presented some examples of the application of our program. Because our program can solve multiple sources simultaneously, the full range Green's function, $G(\tau, \mu, \phi; \tau', \mu', \phi')$, can be computed very efficiently. The distribution of any particular radiative effect is then just a convolution of the Green's function with the source.

Acknowledgements

This work was supported by the Earth Observation Center, CSIRO, Australia and Australian International Postgraduate Research Scholarship (IPRS) program.

References

- [1] Qin Y, Box MA, Jupp DLB. Inversion of multi-angle sky radiance measurement for the retrieval of atmospheric optical properties I: algorithm. *J Geophys Res*, 2002, submitted for publication.
- [2] Box MA, Gerstl SAW, Simmer C. Application of the adjoint formulation to the calculation of atmospheric radiative effects. *Beitr Phys Atmos* 1988;61:303–11.
- [3] Box MA, Gerstl SAW, Simmer C. Computation of atmospheric radiative effects via perturbation theory. *Beitr Phys Atmos* 1989;62:193–9.
- [4] Sendra C, Box MA. Retrieval of the phase function and scattering optical thickness of aerosols: a radiative perturbation theory application. *JQSRT* 2000;64:499–515.

- [5] Sendra C. Retrieval of the aerosol scattering parameters using radiative perturbation theory. Ph.D. thesis, University of New South Wales, Australia, 1996, 164pp.
- [6] Holben BN, Eck TF, Slutsker I, Tanre D, Buis JP, Setzer A, Vermote E, Reagan JA, Kaufman Y, Nakajima T, Lavenu F, Jankowiak I, Smirnov A. AERONET—a federated instrument network and data archive for aerosol characterization. *Remote Sensing Environ* 1998;66:1–16.
- [7] Chandrasekhar S. Radiative transfer. New York: Dover, 1950.
- [8] Liou KN. A numerical experiment on Chandrasekhar’s discrete-ordinate method for radiative transfer: application to cloudy and hazy atmospheres. *J Atmos Sci* 1973;30:1303–26.
- [9] Liou KN. Applications of the discrete-ordinate method for radiative transfer to inhomogeneous aerosol atmospheres. *J Geophys Res* 1975;80:3434–40.
- [10] Asano S. On the discrete ordinates method for the radiative transfer. *J Meteoro Soc Japan* 1975;53:92–5.
- [11] Stamnes K, Swanson RA. A new look at the discrete-ordinate method for radiative transfer calculations in anisotropically scattering atmospheres. *J Atmos Sci* 1981;38:387–99.
- [12] Stamnes K, Conklin P. A new multi-layer discrete ordinate approach to radiative transfer in vertically inhomogeneous atmospheres. *JQSRT* 1984;31:273–82.
- [13] Liou KN. An introduction to atmospheric radiation. New York: Academic Press, 1980.
- [14] Twomey S. Green’s function formulae for the internal intensity in radiative transfer computations by matrix–vector methods. *JQSRT* 1985;33:575–9.
- [15] Domanus HM, Cogley AC. A fundamental-source-function formulation of radiative transfer and the resulting fundamental reciprocity relations. *JQSRT* 1974;14:705–22.
- [16] Evans KF, Stephens GL. A new polarized atmospheric radiative transfer model. *JQSRT* 1991;46:413–23.